

RAPID COMMUNICATION

Mechanochemical synthesis of α -Al₂O₃-Cr³⁺ (Ruby) and χ -Al₂O₃Fernando D. Cortes-Vega^{1,2} | Wenli Yang³ | Juan Zarate-Medina² |Stanko R. Brankovic^{3,4} | Hector A. Calderon⁵ | Francisco C. Robles Hernandez^{1,3,4} ¹Department of Mechanical Engineering Technology, University of Houston, Houston, Texas²Instituto de Investigación en Metalurgia y Materiales, Universidad Michoacana de San Nicolás de Hidalgo, Michoacán, México³Department of Materials Science and Engineering, University of Houston, Houston, Texas⁴Department of Electrical and Computer Engineering, University of Houston, Houston, Texas⁵Instituto Politecnico Nacional, ESFM, UPALM, Zacatenco, CDMX, Mexico**Correspondence**

Francisco C. Robles Hernandez and Fernando D. Cortes-Vega, Department of Mechanical Engineering Technology, University of Houston, Houston, TX. Emails: fcrobles@uh.edu and danielcv87@gmail.com

Abstract

In this work we present a unique method to synthesize χ -Al₂O₃ and α -Al₂O₃ doped with Cr³⁺ (ruby). The ruby is synthesized by mechanical milling of pseudoboehmite that is doped in-situ with chromium. The doping is carried by adding chromium sulfate hydrate to an aqueous solution rich in aluminum sulfate hydrate. The pH in the solution is controlled to be between 9 and 10 by using ammonia, which induces the pseudoboehmite precipitation. The Cr³⁺ is added for its remarkable effects on the detectability of ruby emitting luminescent R₁ and R₂ bands that are traceable in Raman spectroscopy. The formation of ruby is detected at milling times as short as 5 hours and increased with the milling time. Ruby phase is further confirmed by means of true atomic resolution Transmission Electron Microscopy (TEM).

1 | INTRODUCTION

Alumina is an abundant ceramic with a wide-range of applications from cooking to electronics, aerospace, automotive, and defense.^{1–3} This is mainly attributed to its hardness and high-temperature characteristics. Alumina is ideal for coatings for extreme conditions and opto-electronics.⁴ It is known that the binary system Al₂O₃-Cr₂O₃ forms a complete solid solution by the octahedral substitution of Al³⁺ for Cr³⁺. The resulting solid solution is commonly known as ruby.^{5–7} Ruby is known as a gemstone; however, it has remarkable applications in physics, opto-electronics, spintronics, fluorescent target for biomolecular imaging, and lasers.^{8–11} Ruby lasers exhibit a characteristic

long optical emission, in the millisecond range, that involves electron transitions between the electronic states ⁴A₂, ⁴T₂, and ²E. This phenomena is responsible for the sharp resonant bands R₁ and R₂, which are susceptible to residual stresses and temperature.^{12–14} For those characteristics, ruby has emerged as desirable pressure and temperature sensor.¹⁵ Conventionally, ruby is synthesized at temperatures as high as 1200°C,^{10,16} and recently we demonstrated its potential synthesis at lower temperatures (<1000°C).¹⁷

In the present communication, we report a new method for the synthesis of ruby at room temperature; this includes high-energy milling and pseudoboehmite doped with Cr³⁺ as starting powder. Here, it is demonstrated the effective synthesis of χ -Al₂O₃ and α -Al₂O₃+Cr³⁺ (ruby) at room temperature purely by high-energy milling (0–50 h). The precursor materials are raw pseudoboehmite doped with

Fernando D. Cortes-Vega and Wenli Yang with equal contribution, and listed in alphabetic order.

chromium. Our hypothesis is that ruby synthesis takes place by the mechanical substitution of the host aluminum atoms by Cr^{3+} ions. The characterization and identification of ruby is mainly carried by Raman spectroscopy and further confirmed by true atomic resolution transmission electron microscopy (TEM).

2 | EXPERIMENTAL PROCEDURE

2.1 | Synthesis of pseudoboehmite doped with chromium

Chromium doped pseudoboehmite was synthesized by using deionized water, aluminum sulfate hydrate ($\text{Al}_2(\text{SO}_4)_3 \cdot \text{XH}_2\text{O}$, purity $\geq 98\%$ from Sigma Aldrich, St. Louis, MO) and chromium sulfate hydrate ($\text{Cr}_2(\text{SO}_4)_3 \cdot \text{XH}_2\text{O}$ from Sigma Aldrich). Initially, the specific amounts of both sulfates were dissolved in deionized water using a weight ratio of 99.1:0.09 for $\text{Al}_2(\text{SO}_4)_3$ and $(\text{Cr}_2(\text{SO}_4)_3 \cdot \text{xH}_2\text{O})$ respectively. The mixing process was carried out under vigorous stirring and constant temperature of 60°C . This solution was subjected to an ammonia gas (NH_3) treatment to reach a constant pH between 9 and 10. The precipitates of the reaction were filtered and washed with deionized warm water several times. Subsequently, the product was dried at 100°C for 24 hours, which yielded a slightly purple powder.

2.2 | Mechanical milling

Ruby is produced by milling the pseudoboehmite-chromium doped powders. The milling is carried out from 0 to 50 hours in a high-energy Spex mill with sets of five steels

balls, two of 12.5 mm and three of 6 mm. The milling load was of 10 g with no control agent.

2.3 | Characterization

Characterization was carried out by means of XRD (X-ray diffraction) in a Rigaku Smart Lab SE Multipurpose X-Ray Diffraction system with $\text{Cu-K}\alpha$ radiation ($\lambda = 1.5418 \text{ \AA}$). The Raman spectroscopy was conducted on an XploraTM Horiba JY using 532 and 638 nm excitation sources. For Raman measurements the as-milled powders were placed onto a glass substrate and lightly pressed onto another glass substrate to flatten the sample's surface. The atomic resolution transmission electron microscopy imaging was carried in the TEAM 0.5 microscope with aberration-correction at 80 kV with a spherical aberration coefficient of -0.015 mm and a focus spread of $\sim 10 \text{ \AA}$ under low dose conditions. The dose rate is $\sim 20 \text{ e}^-/\text{\AA}^2\text{s}$ for images in focal series of 40 images. The focal series reconstruction was carried using the software MacTempas[®] (Berkeley, CA). This procedure produces phase and amplitude images with atomic resolution.

3 | RESULTS AND DISCUSSION

Figure 1A shows the XRD characterization for the raw and milled samples for up to 50 hours. These results suggest that the complete transformation to $\chi\text{-Al}_2\text{O}_3$ take place between 30 and 50 hours of milling. The reaction rate is a function of the ratio: mass:milling media:milling severity. In other words, similar results can be accomplished at different times

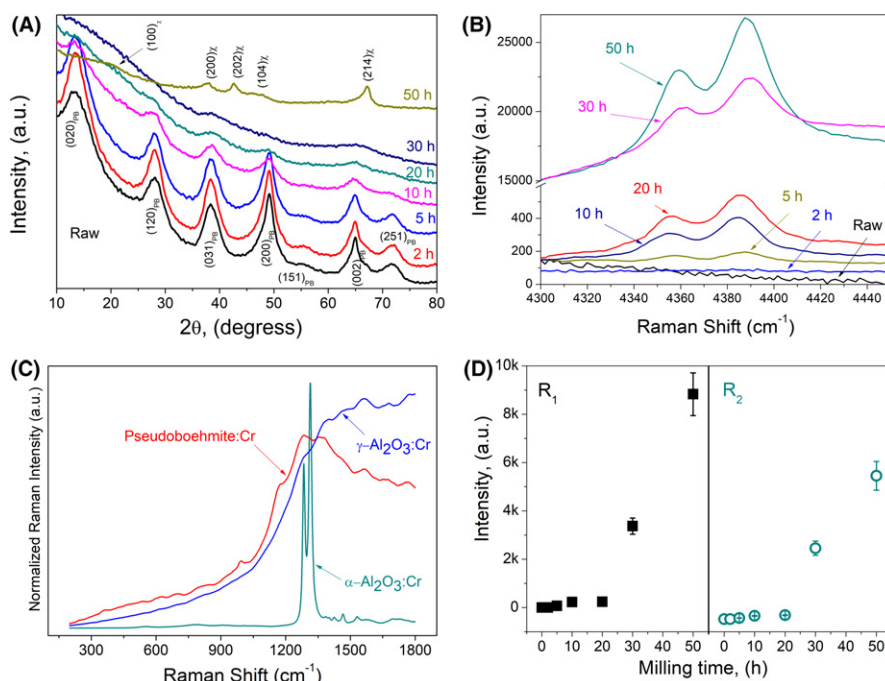


FIGURE 1 Characterization of the raw and milled material by means of (A) XRD and (B) Raman. The subindex PB and χ stand for pseudoboehmite and chi-alumina ($\chi\text{-Al}_2\text{O}_3$) respectively. In (C) are compared the Raman spectra of pseudoboehmite, $\gamma\text{-Al}_2\text{O}_3$ and $\alpha\text{-Al}_2\text{O}_3$ and in (D) is compared the increase on the Raman intensity for the R_1 and R_2 bands as a function of milling time

using alternative conditions. After 10 hours of milling the XRD reflections of pseudoboehmite become shorter and wider. Further milling (20 and 30 hours) shows a further widening of the reflection peaks that can be associated to transformation of the original components, the loss of material crystallinity and a reduction in grain size. After 50 hours of milling the chemical transformation is finished and the sample shows a new set of reflections corresponding to χ - Al_2O_3 with no traceable evidence of pseudoboehmite. The χ - Al_2O_3 is identified using the 13-0373 JCPDS chart. Other reports have also demonstrated the successful synthesis of χ - Al_2O_3 and α - Al_2O_3 by milling.^{18,19} However, to the best of our knowledge there are no reports of room-temperature synthesis of ruby, except for our previous work where we

use two precursors (pseudoboehmite and Cr_2O_3),¹⁷ instead of pure Cr-doped pseudoboehmite. The formation of χ - Al_2O_3 is evident from XRD, however, to identify α - Al_2O_3 we resorted to use Raman. In a parallel research we have demonstrated that ruby can be produced by milling pure pseudoboehmite and pure chromium oxide (Cr_2O_3).¹⁷ In the current work we start with Cr-doped pseudoboehmite.

The XPS and XDR techniques show no traces of Fe. Fe contamination during mechanical milling is normally found in other reports including our previous work.¹⁷⁻¹⁹ Nevertheless now it has been clearly reduced due to the soft nature of the precursors in use.

Figure 1B displays the Raman spectra of the raw and milled samples. The presence of ruby phase is clearly

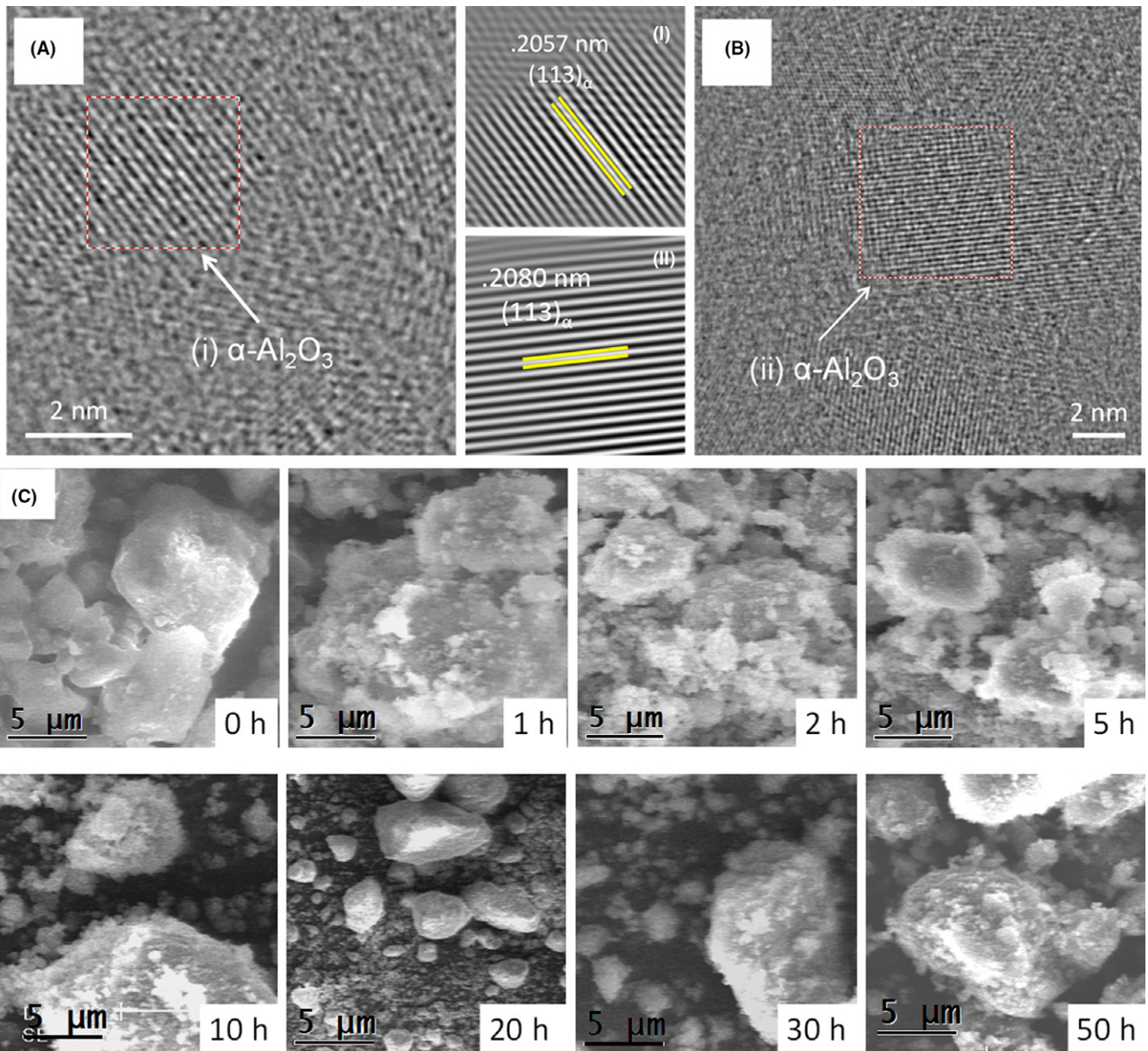


FIGURE 2 A,B, True Atomic Resolution (TEM) images and interplanar measurements for the 20 hours and 30 hours milled samples, and C, SEM microstructures of the raw and milled samples for up to 50 hours

identified by its characteristic luminescent Raman bands R_1 and R_2 . They are observed in the frequency range of 4300 cm^{-1} - 4500 cm^{-1} for a 532 nm excitation. Figure 1B shows that the intensity of the ruby phase bands increases with milling time up to 50 hours. This is associated to the increasing amount of transformed ruby. Figure 1B shows the change in the intensity of both resonant ruby bands as a function of milling time and in combination with the XRD results of Figure 1A, it can be concluded, that this is due to a higher degree of crystallinity.

The crystallinity of ruby has been directly related to the luminescent bands R_1 and R_2 .²⁰ Moreover, the only alumina phase having the R_1 and R_2 bands is $\alpha\text{-Al}_2\text{O}_3$ and those bands have never been associated with any other Al_2O_3 phase (eg $\chi\text{-Al}_2\text{O}_3$, $\delta\text{-Al}_2\text{O}_3$ and $\theta\text{-Al}_2\text{O}_3$, pseudoboehmite, etc.). In order to prove this, the raw material (rich in pseudoboehmite) was heat treated to synthesize pure $\gamma\text{-Al}_2\text{O}_3$. The corresponding Raman spectra of both samples are compared with that of $\alpha\text{-Al}_2\text{O}_3$ in Figure 1C. The absence of the R_1 and R_2 bands in the raw and synthesized materials could not be attributed to the lack of Cr. This is because all investigated samples were synthesized using the same raw material; therefore, the absence of the R_1 and R_2 bands is not the result of a lack of Cr. Figure 1C demonstrates that the luminescent bands R_1 and R_2 are inherent only to the presence of $\alpha\text{-Al}_2\text{O}_3$. In contrast with the sharp bands exhibited by ruby ($\text{Cr}^{3+}\text{-}\alpha\text{-Al}_2\text{O}_3$); the pseudoboehmite and $\gamma\text{-Al}_2\text{O}_3$ show only broad bands. This further demonstrates that our process is effective to produce ruby as confirmed in Figure 1B.

The amount of synthesized ruby is tunable and increases with milling time as seen by the change in the intensity of the resonant bands R_1 and R_2 for this phase (Figure 1D). The intensity of R_1 and R_2 bands from the raw sample to the sample milled for 20 hours increases linearly. However, the samples milled for 30 hours and 50 hours show an abrupt (exponential) increase in intensity. It is likely that the synthesis of $\chi\text{-Al}_2\text{O}_3$ and $\alpha\text{-Al}_2\text{O}_3$ occurs by the elimination of water in pseudoboehmite due to milling at early processing times. The phase transformation from pseudoboehmite to $\chi\text{-Al}_2\text{O}_3$ and $\alpha\text{-Al}_2\text{O}_3$ occurs due to localized high-pressures exerted on the material by the individual ball collisions.

In Figures 2A,B shows true atomic resolution TEM phase images for the samples milled for 20 hours and 30 hours respectively. The analysis of interplanar measurements provides further evidence that confirms the successful synthesis of the crystalline $\alpha\text{-Al}_2\text{O}_3$ in both samples. The grain size determination by means of Scherrer shows values between 4 and 7 nm for the investigated samples, which is in agreement with true atomic resolution TEM. The grain size calculated from Scherrer formula provides a bulk assessment while the electron microscopy presented herein is rather discrete investigation of the grain size. It is important to consider that this


is purely a reference number as the Scherrer calculation does not account for residual stresses and therefore its validity is compromised. Yet, in a rapid comparison, one can see that the particles observed by TEM are in the same range as the results obtained using XRD analysis.

The SEM shows the particle size for the raw sample is homogeneous ranging in the micrometric scale. All milled samples have a bimodal particle distribution. The large particles are $>5\text{ }\mu\text{m}$ and smaller particles usually below $5\text{ }\mu\text{m}$ to submicrometric. The larger particles reach sizes of up to $50\text{ }\mu\text{m}$. The subnanometric particles are most-likely debris due to the milling process. The morphology in all cases is irregular and each particle is formed by clusters of nanostructures as demonstrated by XRD and TEM.

4 | CONCLUSION

Here, it is introduced a new method for the room-temperature synthesis of ruby from Cr^{3+} -doped pseudoboehmite purely by milling. Mechanical milling supplies sufficient energy to transform the pseudoboehmite into $\chi\text{-Al}_2\text{O}_3$ that is later transformed into Cr^{3+} -doped $\alpha\text{-Al}_2\text{O}_3$ or ruby. The ruby phase is identified with Raman spectroscopy and its existence is then confirmed by true atomic resolution TEM. The major novelty of our work is the introduction of a simple and low cost technique to produce nano-ruby powders by using pseudoboehmite doped with Cr^{3+} as precursor. The nano-ruby presents an exceptional opportunity for a wide range of advanced applications from electronics to bio and medical uses.

ORCID

Francisco C. Robles Hernandez  <http://orcid.org/0000-0001-5587-0802>

REFERENCES

1. Masuda H, Asoh H, Watanabe M, Nishio K, Nakao M, Tamamura T. Square and triangular nanohole array architectures in Anodic Alumina. *Adv Mater.* 2001;13(3):189–92.
2. Trimm DL, Stanislaus A. The control of pore size in alumina catalyst supports: a review. *Appl Catal.* 1986;21(2):215–38.
3. Trueba M, Trasatti SP. γ -Alumina as a support for catalysts: a review of fundamental aspects. *Eur J Inorg Chem.* 2005;2005(17):3393–403.
4. Chang S, Doremus RH, Schadler LS, Siegel RW. Hot-pressing of nano-size alumina powder and the resulting mechanical properties. *Int J Appl Ceram Technol.* 2004;1(2):172–9.
5. Rastorguev A, Baronskiy M, Zhuzhgov A, Kostyukov A, Krivoruchko O, Snytnikov V. Local structure of low-temperature $\gamma\text{-Al}_2\text{O}_3$ phases as determined by the luminescence of Cr^{3+} and Fe^{3+} . *RSC Advances.* 2015;5(8):5686–94.

6. Maiman TH. Stimulated optical radiation in ruby. *Nature*. 1960;187:493.
7. Yamaoka H, Zekko Y, Jarrige I, Lin J-F, Hiraoka N, Ishii H, et al. Ruby pressure scale in a low-temperature diamond anvil cell. *J Appl Phys*. 2012;112(12):124503.
8. Fünfer E, Kronast B, Kunze HJ. Experimental results on light scattering by a θ -pinch plasma using a ruby laser. *Phys Lett*. 1963;5(2):125–7.
9. Birks LS, Hurley JW, Sweeney WE. Perfection of ruby laser crystals. *J Appl Phys*. 1965;36(11):3562–5.
10. Edmonds AM, Sobhan MA, Sreenivasan VKA, Grebenik EA, Rabeau JR, Goldys EM, et al. Nano-ruby: a promising fluorescent probe for background-free cellular imaging. *Part Part Syst Charact*. 2013;30(6):506–13.
11. Sreenivasan VKA, Wan Razali WA, Zhang K, Pillai RR, Saini A, Denkova D, et al. Development of bright and biocompatible nanoruby and its application to background-free time-gated imaging of G-protein-coupled receptors. *ACS Appl Mater Interfaces*. 2017;9(45):39197–208.
12. Syassen K. Ruby under pressure. *High Press Res*. 2008;28(2):75–126.
13. Jovanic BR. Lifetime of the ruby R1 line under ultrahigh pressure. *Chem Phys Lett*. 1992;190(5):440–2.
14. Ma D-p, Zheng X-t, Xu Y-s, Zhang Z-g. Theoretical calculations of the R1 red shift of ruby under high pressure. *Phys Lett A*. 1986;115(5):245–8.
15. Fals AE, Hadjiev VG, Robles Hernández FC. Multi-functional fullerene soot/alumina composites with improved toughness and electrical conductivity. *Mat Sci Eng: A*. 2012;558:13–20.
16. Bulyarskii SV, Kozhevin AE, Mikov SN, Prikhodko VV. Anomalous R-line behaviour in nanocrystalline $\text{Al}_2\text{O}_3\text{:Cr}^{3+}$. *physica status solidi (a)*. 2000;180(2):555–60.
17. Cortes-Vega FD, Yang W, Zarate-Medina J, Brankovic SR, Herrera Ramírez JM, Robles Hernandez FC. Room-temperature synthesis of $\chi\text{-Al}_2\text{O}_3$ and ruby ($\alpha\text{-Cr:Al}_2\text{O}_3$). *CrystEngComm*. 2018;20(25):3505–11.
18. Tonejc A, Bagovic D, Kosanovic C. Comparison of the transformation sequence from [g]-AlOOH (Boehmite) to [a]- Al_2O_3 (Corundum) Induced by Heating and by Ball Milling 1994. *Mater. Sci. Eng*. 1994;A181/A182:1227–231.
19. Kozawa T, Naito M. Mechanically induced formation of metastable χ - and $\kappa\text{-Al}_2\text{O}_3$ from boehmite. *Adv Powder Technol*. 2016;27(3):935–9.
20. Patra A, Tallman RE, Weinstein BA. Effect of crystal structure and dopant concentration on the luminescence of Cr^{3+} in Al_2O_3 nanocrystals. *Opt Mater*. 2005;27(8):1396–401.

How to cite this article: Cortes-Vega FD, Yang W, Zarate-Medina J, Brankovic SR, Calderon HEA, Robles Hernandez FC. Mechanochemical synthesis of $\alpha\text{-Al}_2\text{O}_3\text{-Cr}^{3+}$ (Ruby) and $\chi\text{-Al}_2\text{O}_3$. *J Am Ceram Soc*. 2018;00:1–5. <https://doi.org/10.1111/jace.16171>